Electric circuit analysis for plasma breakdown in JT-60SA

Kunihito YAMAUCHI[1)], Katsuhiro SHIMADA[1)], Tsunehisa TERAKADO[1)], Makoto MATSUKAWA[1)], Philippe CARA[2)], Elena GAIO[3)], Maurizio SANTINELLI[3)], Roberto COLETTI[4)] and Alberto COLETTI[5)]

[1)] *Japan Atomic Energy Agency, Naka, Ibaraki, Japan*

[2)] *CEA, IRFM, Cadarache, Saint-Paul-lez-Durance, France*

[3)] *Consorzio RFX, Euratom-ENEA Association, Padova, Veneto, Italy*

[4)] *ENEA, Frascati, Rome, Italy*

[5)] *Fusion for Energy, Garching, Bavaria, Germany*

(Received: 30 October 2009 / Accepted: 13 February 2010)

To obtain stable plasma breakdown and for designing the details of a power supply system in JT-60SA, a precise evaluation of the magnetic field performance using an accurate circuit analysis model has to be conducted. This evaluation should include AC/DC converters such as thyristor converters and a high voltage generation circuit which consists of a DC current interrupter and a resistor set. In this paper, the preparation procedure of the analysis model is presented. Using this modeling method, a circuit analysis including not only complex interactions but also nonlinear phenomenon can be performed. As one of the applications of it, a circuit analysis of the tokamak system JT-60SA is demonstrated using the PSIM code. Specifically, some circuit analysis results of plasma breakdown at t=0−60 ms are shown using an ideal voltage source and a thyristor converter model for comparison. Then, the voltage fluctuations of the generator (H-MG, 400 MVA) at plasma initiation and their influence are also described.

Keywords: JT-60SA, breakdown, circuit analysis, passive coil model, converter, generator, PSIM

1. Introduction

A high current of about 500 kA will be induced in the passive structures such as the vacuum vessel and the stabilizing plate at plasma initiation in JT-60SA [1], because the total electric resistance of the passive structures is approximately 16.5 μΩ and the breakdown electric field of 0.5 V/m is expected for stable plasma initiation from the experiments of JT-60U [2]. Therefore, a precise evaluation of the magnetic field performance using an accurate circuit analysis model has to be possible, and must be conducted to obtain stable plasma breakdown and for designing the details of a power supply system. This evaluation should include AC/DC converters such as thyristor converters and a high voltage generation circuit which consists of a DC current interrupter and a resistor set.

In this paper, the preparation procedure of the analysis model is presented. Using this modeling method, a circuit analysis including not only complex interactions but also nonlinear phenomenon can be performed. As one of the applications of it, a circuit analysis of the tokamak system JT-60SA is demonstrated using the PSIM[†] code. The purpose of the circuit analysis is to obtain stable plasma breakdown and for designing the details of a power supply system in JT-60SA. Specifically, some circuit analysis results of plasma breakdown at t=0−60 ms are shown using an ideal voltage source and a thyristor converter model for comparison. The delay effect on the converter voltage control is summarized as the first achievement. The voltage fluctuations of the generator (H-MG, 400 MVA) at plasma initiation are also described, because large reactive power fluctuations may cause large voltage fluctuations and sudden phase shifts of the AC voltage supplied by H-MG and consequently applied to the thyristor converters.

[†] PSIM is a simulation software designed for power electronics, motor control, and dynamic system simulation. (Powersim Inc.: http://www.powersimtech.com/)

2. Configuration of JT-60SA Coil Power Supplies

Figure 1 shows a schematic circuit diagram of the AC power system for Poloidal Field (PF) coils. In JT-60SA, there are ten superconducting PF coils, i.e. four Central Solenoids (CS) and six Equilibrium Field (EF) coils, and they are energized by the motor-generator (H-MG) through AC/DC converters. H-MG is reused from JT-60, and consists of a synchronous generator, a flywheel and an induction motor for driving. The main specification of H-MG is shown in Table 1. There are two kinds of AC/DC converter for the PF coils. One is the low voltage

author's e-mail: yamauchi.kunihito@jaea.go.jp

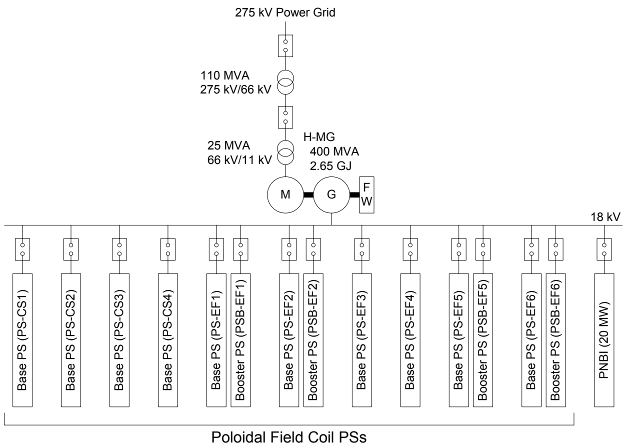

Fig. 1 Schematic circuit diagram of AC power system for Poloidal Field (PF) coils.

thyristor converter (±1 kV, ±20 kA) with continuous rating, and is named as Base PS. Another is the high voltage thyristor converter (±5 kV, +4/−14.5 kA) with short-time rating, and is reused from Vertical field coil PS (PSV) in JT-60. In JT-60SA, it is renamed as Booster PS (PSB). Though Base PS is used for all the PF coils, Booster PS is utilized for EF1, 2, 5 and 6 coils only.

Figures 2 and 3 show schematic DC circuit diagrams of the typical PF coil PSs with Booster PS and with Switching Network Unit (SNU), respectively. SNU is involved in the PF coil PSs without Booster PS, and is a high voltage generator (–5 kV) that consists of a DC current interrupter and a resistor set. Unlike Booster PS powered by H-MG directly, SNU is workable with using the energy stored in the PF coil. Both Booster PS and SNU can be basically operated to obtain a high voltage for short duration of plasma breakdown and initiation. Therefore, the PF coils are driven by Base PSs for most of the operation period including the pre-magnetization and plasma current flat-top phases.

Table 1 Main specification of H-MG

Rated capacity	400 MVA
Rated voltage	18 kV
Rated current	12830 A
Frequency	77.6–54.2 Hz
Rotating speed	582–406.5 rpm
Available discharge energy	2650 MJ
Drive type	Induction motor drive

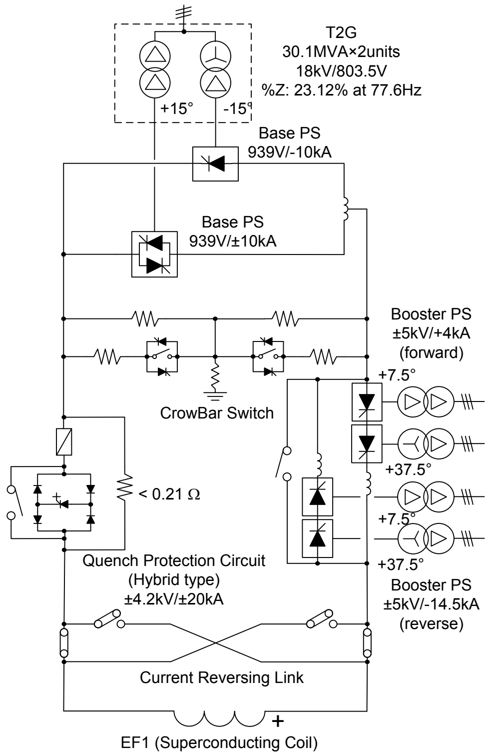

Fig. 2 Schematic DC circuit diagram of EF1 coil PS (Typical PF coil PS with PSB).

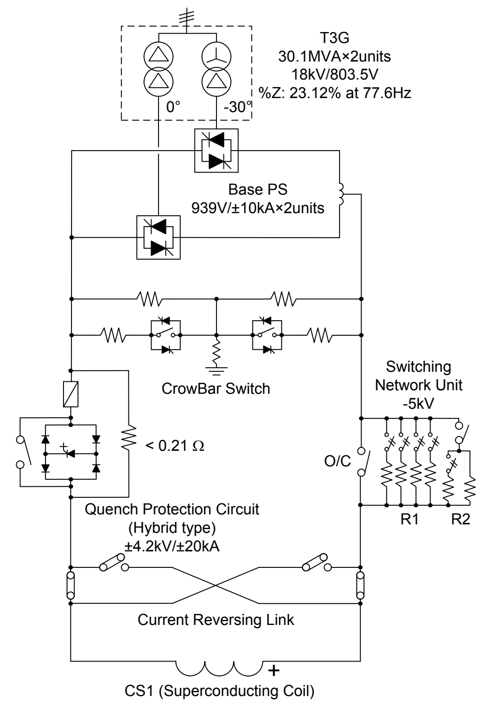

Fig. 3 Schematic DC circuit diagram of CS1 coil PS (Typical PF coil PS with SNU).

3. Analysis Model

3.1. Modeling of PF Coils

Since the PF coils are magnetically coupled with not only other PF coils but also many conductor elements such as the vacuum vessel and the stabilizing plate, their interactions should be included. Of course, the plasma is also coupled with them magnetically. But, it is not necessary to be considered at the plasma breakdown phase because there is no plasma.

Assuming axial symmetry of tokamak device, the passive structures could be represented as an assembly of about 120 thin passive poloidal field coils in order to calculate their induced eddy current [2]. However, there

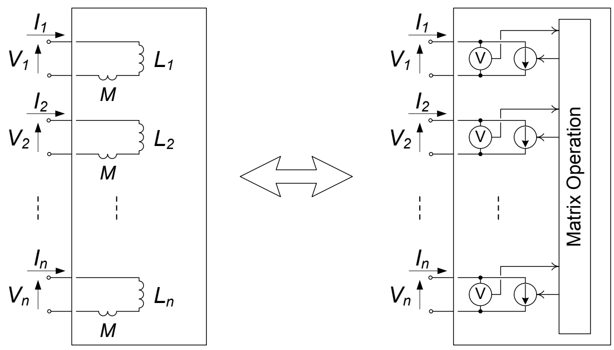

Fig. 4 Multiple coil circuit model based on current source equivalent circuit.

is no easily available circuit model applicable to such a multiple coil with magnetic coupling in the conventional circuit analysis code. In fact, a calculation of 130 mutually coupled coils (10 PF and 120 passive coils) can not be achieved using the built-in circuit elements in the conventional codes such as PSIM (six coupled inductors at most) and PSCAD/EMTDC‡ (no such an element). In addition, although the number of the passive coils was chosen as 120 in this case from the experience considering the stability of numerical analysis and the viewpoint of shortening the calculation time, the model of the passive structures can be further divided into more passive coils for high precision.

To solve this problem, we have utilized a very conventional and ideally flexible circuit element, i.e. externally controlled current source. Figure 4 indicates the multiple coil circuit model based on the current source equivalent circuit. The process is as follows;

(1) Observing the applied voltage at the terminals of coils

(2) Deriving the supplied magnetic flux $\boldsymbol{\Psi}$ (= voltage-time product) into each coil by the numerical integration of the observed voltages

(3) Providing the coil current value $\boldsymbol{I}$ to the externally controlled current source using the equation of $\boldsymbol{\Psi} = \boldsymbol{LI}$.

Here, $\boldsymbol{L}$ is the inductance matrix. Practically the coil currents can be calculated by the following equation;

$$\begin{aligned} I_n &= \sum_{i=1}^{130} M_{ni} \int V_i dt \\ &= I_{n\_prev} + \sum_{i=1}^{130} M_{ni} \frac{V_i + V_{i\_prev}}{2} \Delta t \qquad (1) \end{aligned}$$

where M_{ni} is the 130×130 susceptance matrix for the 10 PF and 120 passive coils, and I_{n_prev} and V_{i_prev} are the current and voltage values at the previous time step, respectively. As for the 120 passive coils, the terminal voltage is calculated from the resultant current value and the resistance matrix, and is internally used to the current calculation at the next time step.

In the case of PSIM, such a process was realized by several control blocks using C language. While, the similar technique is possible using Fortran in the case of PSCAD/EMTDC. The developed model has the following merits;

(a) Sensitivity study of the circuit parameter is easy.

(b) Geometry of the passive structures can be quickly updated.

(c) Expansion to more advanced model which can involve the plasma behavior such as position and shape could be possible.

In this paper, the PF coils and the passive structures with magnetic coupling in JT-60SA are modeled. However, using this modeling method, a circuit analysis including not only complex interactions but also nonlinear phenomenon can be performed.

3.2. Modeling of Coil Power Supplies

Figure 5 shows the DC circuit diagram of the PSIM simulation model for a plasma breakdown analysis. In this analysis model, Base PSs with CrowBar circuit are bypassed for simplicity because Booster PSs and SNUs are working during plasma breakdown. Similarly, Quench Protection Circuits (QPCs) are also bypassed for simplicity since they works in the case of a superconducting coil quench or a PS apparatus failure.

For modeling of SNUs, ideal switches are used as the DC circuit interrupters, and all of them open together at t=0 ms. The resistance value of each SNU is properly

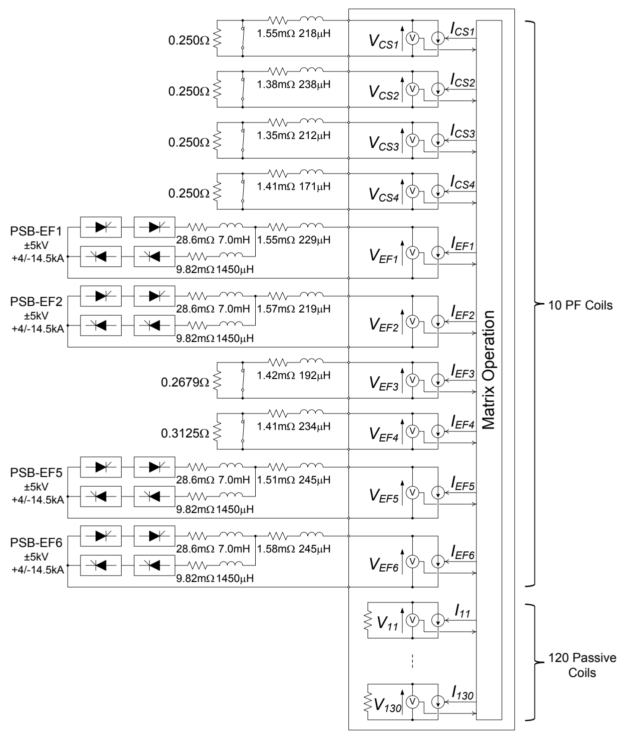

Fig. 5 DC circuit diagram of PSIM simulation model for plasma breakdown analysis.

‡ PSCAD is a power system simulation software for the design and verification of all types of power systems. EMTDC is the simulation engine, which is now the integral part of PSCAD graphical user interface. (Manitoba HVDC Research Centre Inc.: https://pscad.com/)

selected by the used scenario.

Booster PS consists of forward and reverse two-quadrant thyristor converters. To provide the smooth coil current zero crossing, a circulating current operation is utilized. Therefore, to reduce the ripples of the circulating current between the forward and reverse converters, DC reactors are attached to Booster PS.

As for other circuit elements, some resistances and inductances, such as DC feeders of about 440 m between the PF coils and their PS components, are considered.

3.3. Modeling of AC Power System

In JT-60SA, the thyristor converters for the PF coils are powered by H-MG. Unlike the power grid system, the frequency varies momentarily because the rotating speed of H-MG depends on the rotational kinetic energy stored in the rotor with the flywheel. Especially in plasma breakdown phase, large reactive power fluctuations may cause large voltage fluctuations and sudden phase shifts of the AC source voltage for the thyristor converters. Therefore, it is important to model H-MG for realistic analysis.

For modeling of H-MG, the built-in circuit element of 3-phase synchronous machine with external excitation is applied. The H-MG machine is accelerated to the rated maximum rotating speed before the operation start (t=0 ms), and then provides power by converting the rotational kinetic energy into electric energy. In addition, a mechanical load element is used to represent the flywheel effect of the H-MG rotor and the total mechanical losses due to friction and windage that is assumed as the constant torque at the rated maximum rotating speed. To follow the momentarily varying frequency of H-MG, a vector phase-locked loop (PLL) is modeled for synchronization. The output voltage of H-MG is controlled by PI feedback regulation at 18 kV with the external excitation circuit.

Phase-shifting converter transformers (–7.5°, +7.5°, +22.5° and +37.5° for Booster PSs) are used in order to suppress harmonics in the H-MG power line. Therefore, they are also modeled using multiple built-in single-phase transformer elements.

3.4. Control Method

For the control of Booster PS, a feedforward control system is applied for fast response. Figure 6 indicates the block diagram of the feedforward control for Booster PS.

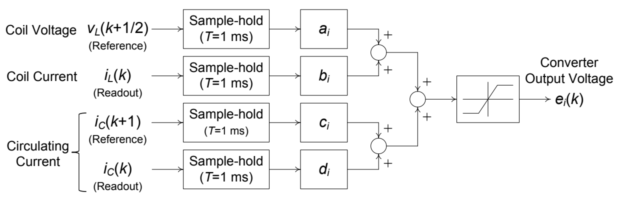

Fig. 6 Block diagram of feedforward control for Booster PS.

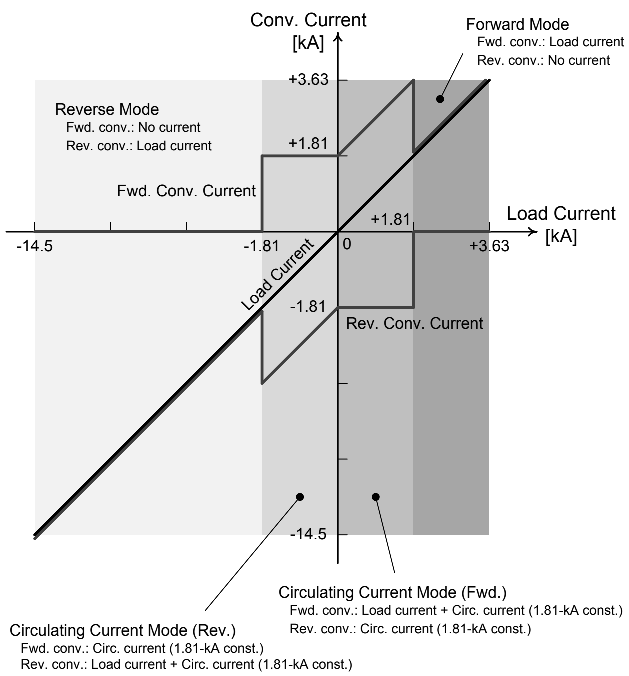

Fig. 7 Diagram of circulating current control mode for Booster PS.

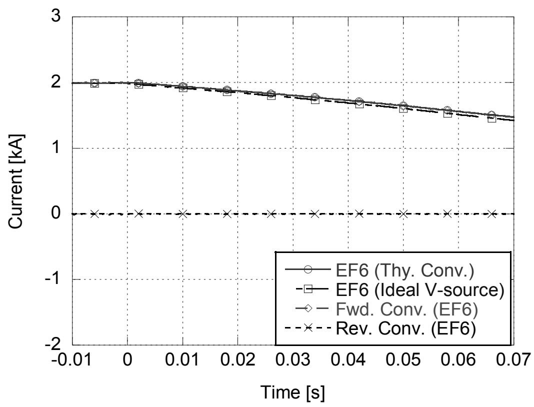

Fig. 8 Current waveforms of EF6 coil and thyristor converters.

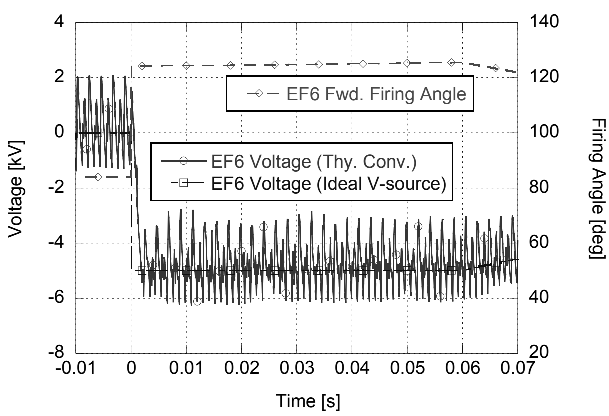

Fig. 9 Waveforms of EF6 coil voltage and firing angle for thyristor converters.

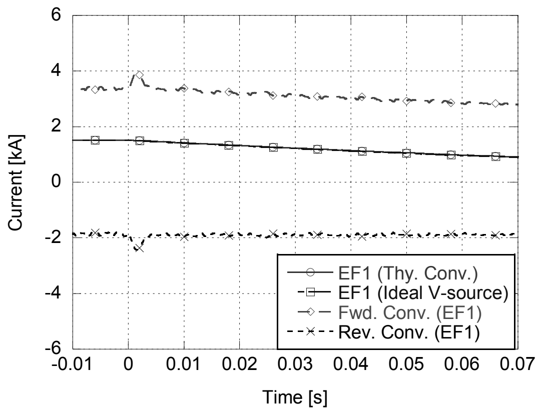

Fig. 10 Current waveforms of EF1 coil and thyristor converters.

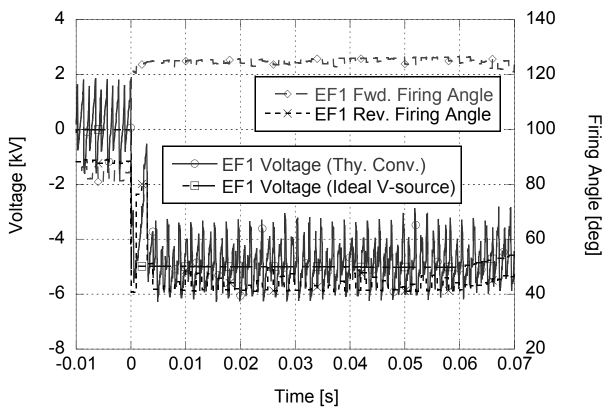

Fig. 11 Waveforms of EF1 coil voltage and firing angle for thyristor converters.

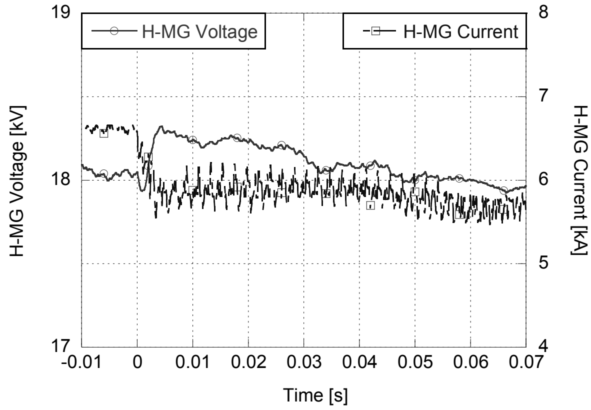

Fig. 12 Waveforms of AC voltage and current supplied by H-MG.

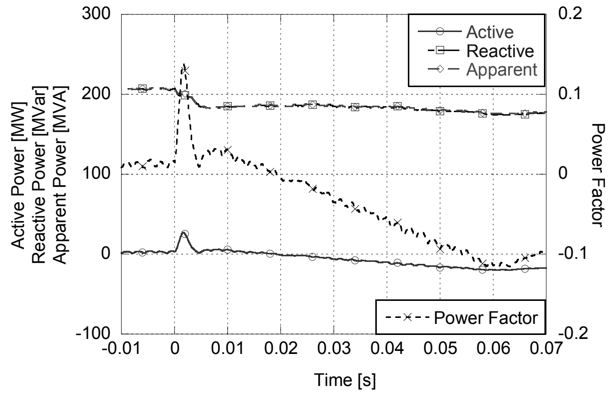

Fig. 13 Waveforms of AC power supplied by H-MG and power factor.

This system is based on the circuit equations, and the control constants were also derived from the circuit parameters. The coil voltage is controlled via the converter output voltage during plasma breakdown. To provide the smooth coil current zero crossing, a circulating current between the forward and reverse converters is simultaneously controlled according to the coil current as shown in Fig. 7. Here, both the reference of the circulating current and the positive/negative thresholds of the coil current are fixed at half of the rating of the forward converters because of the asymmetric current rating between the forward and reverse converters. In this model, the periodic control interval is set to 1 ms equal to that in JT-60.

4. Results and Discussion

Using the developed model, a PSIM simulation was performed for the duration of t=0–60 ms corresponding to plasma breakdown phase. The preliminary results are described below.

4.1. Control Response of Thyristor Converter

Figures 8 and 9 show the simulation result of current and voltage waveforms of EF6 coil. In those figures, the result in the case of the ideal voltage sources instead of the thyristor converters are also indicated for comparison. In addition, the current waveforms of the forward and reverse converters of Booster PS for EF6, and the firing angle for the forward converters are also shown for reference. The current waveform in the case of the thyristor converters gives close agreement with that in the case of the ideal voltage source. This agreement is contributed by the fast response of the feedforward control. However, it is found that the converter voltage control is delayed for approximate 2 ms in compared with the ideal voltage source, and this delay leads to the discrepancy between the current waveforms of the thyristor converters and the ideal voltage source. At the initial coil current of EF6 (1.99 kA), Booster PS is operated in Forward Mode with no circulating current. In this situation, since only the forward converters are working, the control response to the step input from small firing angle to large one is slow due to the natural commutation.

Such a control delay can be also observed in Fig. 11. In this case, Booster PS for EF1 is operated in Circulating Current Mode. Therefore, the control response depends on both of the forward and reverse converters. Is this situation, the step response of the forward converters is slow as in the above-mentioned case, and that of the reverse ones is fast. In Fig. 10, it is found that an overshoot of the circulating current appears at t=0 ms. This overshoot also implies the unbalance response between the forward and reverse converters.

4.2. AC Voltage and Power

Figure 12 shows the waveforms of the AC voltage and current supplied by H-MG. Although the output voltage of H-MG is controlled by PI feedback regulation at 18 kV, it is found that the voltage fluctuations are caused by the rapid load change started at t=0 ms and the internal impedance.

Figure 13 indicates the waveforms of the AC power supplied by H-MG and the power factor. An apparent power of about 200 MVA is observed and the reactive power is strongly dominant. This result is half the rated capacity of H-MG, however, is based on the case of no Base PSs. Actually, a higher reactive power must be observed. Therefore, for evaluation of the reactive power and the voltage drop, a further circuit analysis including Base PSs has to be conducted.

5. Conclusions

Using the modeling method mentioned in this paper, a circuit analysis including not only complex interactions but also nonlinear phenomenon can be performed. As one of the applications of it, a circuit analysis of the tokamak system JT-60SA was demonstrated using the PSIM code.

The purpose of the circuit analysis is to obtain stable plasma breakdown and for designing the details of a power supply system in JT-60SA. Some simulation results of plasma breakdown at t=0–60 ms were preliminarily shown using an ideal voltage source and a thyristor converter model for comparison. As a result, the delay effect of the converter voltage control was summarized as the first achievement. Furthermore, the voltage fluctuations of H-MG at plasma initiation and their influence were also described.

As future works, some modifications are required to complete the modeling such as Base PSs and SNUs. Specifically, for evaluation of the reactive power and the voltage drop at H-MG, a circuit analysis including Base PSs has to be performed. In addition, a realistic modeling of the DC current interrupter in SNU has to be conducted to investigate the influence of the delay and jitter. Ultimately, the plasma should be involved for analyzing and designing the details of a power supply system such as protection sequence in the case of a plasma disruption.

Acknowledgements

This work was supported within the framework of the “Broader Approach Internationals Agreement”.

References

[1] M. Matsukawa *et al*., “Status of JT-60SA tokamak under the EU-JA Broader Approach Agreement”, *Fusion Eng. Des.*, **83**, 795–803 (2008).

[2] M. Matsukawa *et al*., “Optimization of plasma initiation scenarios in JT-60SA”, *APFA 2009* (to be published in *JPFR Series*).